International Journal of Environmental Science and Technology (2026) 23:282
https://doi.org/10.1007/s13762-026-07084-6

ORIGINAL PAPER

Vanadium removal from water assisted by $FeCl_3$ using low pressure membranes

O. K. Turk[1] · **M. Cakmakci**[1] · **F. Acar**[1]

Received: 20 January 2025 / Revised: 25 December 2025 / Accepted: 18 January 2026
© The Author(s) 2026

Abstract

Vanadium (V), released from both natural and anthropogenic sources, occurs in groundwater and surface waters at 0.2–100 µg L^{-1} (freshwater) and 0.2–29 µg L^{-1} (seawater). This work evaluates V removal with low-pressure membranes (MV020 and UP150) enhanced with $FeCl_3$. The effects of Fe/V molar ratio, transmembrane pressures (TMPs), and membrane type on removal efficiency and flux performance were examined. In a 60-min operational period, V rejection at Fe/V = 0 remained below 61.8% (UP150) and 24.5% (MV020). Raising the ratio at Fe/V = 1 increased removal to 73.9% (UP150) and 53.3% (MV020); at Fe/V = 3 the values rose to 88.3% and 60.2%, respectively. In 6-h operational period with UP150 at Fe/V = 3, peak removal reached 95.1%, but progressive fouling caused flux decline; after backwashing cycles the flux partially recovered while removal stabilised around 86%. SEM–EDS and FTIR analyses confirmed Fe–V interactions on membrane surfaces. Overall, $FeCl_3$-assisted low-pressure UF offers high V rejection with moderate chemical demand, making it a compact and energy-efficient option for decentralised water treatment.

Keywords Vanadium · Membrane filtration · Drinking water · Low pressure membranes

Introduction

V is a transition metal from the fourth period of the periodic table and is widely distributed in the Earth's crust at an average concentration of approximately 100 mg kg^{-1} (Sefström 1831; Mamane et al. 1998; Barceloux and Barceloux 1999; Cintas 2004; Rehder 2015; Vasseghian et al. 2021). Each year, around 65,000 tons of V are released from natural sources and an additional 200,000 tons are introduced into the environment due to anthropogenic activities such as mining, fuel combustion, and metallurgical processes (ATSDR 2012; Gillio Meina et al. 2019; Gillio Meina 2020). With rising global industrial demand, V consumption has increased by nearly 45% since 2011, reaching 102.1 kilotons in 2019 and was projected to exceed 130 kilotons by the end of 2024. Given its growing prevalence and recognized toxicity, V has been included in the U.S. Environmental Protection Agency's (USEPA) Contaminant Candidate List (CCL), highlighting the need for effective removal strategies in water treatment processes (Lin et al. 2021; Gurjar et al. 2022; Simandl and Paradis 2022; Richardson and Manasfi 2024; Ohwobete et al. 2025).

Various technologies have been developed for V removal from aqueous systems. Among these, adsorption, ion exchange, chemical precipitation, biological treatment, and membrane filtration are commonly studied. Adsorption is widely applied due to its simplicity and efficiency, and recent research reports removal rates of 89.0% on metal–organic frameworks (MOFs) (Ma et al. 2023), 97.1% on basic oxygen furnace (BOF) steel slag (Gao et al. 2017), 98.0% and 100% on Fe-loaded and Zn-loaded biochars (Meng et al. 2018; Dong et al. 2024); fixed-bed systems packed with granular ferric hydroxide (GEH®) consistently reduce dissolved V below 2 µg L^{-1} in full-scale plants (Bahr et al. 2022). Limitations include rapid adsorbent saturation, costly regeneration and competition with co-occurring oxyanions (Zhu et al. 2018; Salehi et al. 2020). Ion-exchange resins achieve > 80% removal in controlled matrices but foul readily and require chemical-intensive regeneration (Al-Jaser and Hamoda 2019; Tan et al. 2023). Chemical precipitation with

Editorial responsibility: Samareh Mirkia.

✉ O. K. Turk
oturk@yildiz.edu.tr

[1] Department of Environmental Engineering, Yildiz Technical University, Davutpasa Campus, 34220 Esenler, Istanbul, Turkey

Published online: 04 February 2026

$FeCl_3$ or $Al_2(SO_4)_3$ is inexpensive and simple but often produces voluminous sludge and leaves residual V at near-neutral pH (Chen et al. 2011; Roccaro and Vagliasindi 2015). Biological approaches such as biosorption on cellulose nanocrystals or anaerobic bio-reduction exhibit promising laboratory-scale performance (~90% removal) yet suffer from slow kinetics and process complexity (Liu et al. 2017; Zulu et al. 2020; Hao et al. 2021).

Membrane technology is becoming increasingly widespread in numerous sectors, such as water treatment, food and beverage processing, pharmaceutical production, and energy generation. Membranes offer a number of advantages over conventional treatment methods, including higher separation efficiency, compact design, and operational simplicity (Judd 2017; Obotey Ezugbe and Rathilal 2020; Rudin et al. 2021; Bera et al. 2022). Membrane filtration can remove a wide range of contaminants, including bacteria, viruses, suspended solids and dissolved substances such as salts, minerals and organic compounds. There are few studies in the literature on the removal of V from water by membrane filtration. Shang et al. investigated V recovery by nanofiltration and found 98% and 96% V rejection in DK and DL membranes, respectively (Shang et al. 2014). Rout and Sarangi reached 99.8% V recovery with a hollow fiber membrane (Rout and Sarangi 2014). Membrane filtration can be an important tool for the removal of some metals such as V. Nevertheless, challenges such as high operating pressures, membrane fouling, and system costs remain barriers to wide adoption (Liu et al. 2022; Peng et al. 2022). To improve economic feasibility, especially in decentralized or small-scale applications, low-pressure membrane systems offer a promising alternative. However, their lower intrinsic rejection rates necessitate process enhancements. In this context, the use of coagulant-assisted membrane filtration, particularly the addition of iron-based salts has emerged as a viable strategy to increase removal efficiencies for metal ions, including V (Shon et al. 2005; Mahdavi et al. 2018; Moreira et al. 2023).

This study investigates the removal of V from water using low-pressure membrane systems, with and without the addition of Fe(III) salts. The objectives are: (i) to evaluate the V rejection efficiency of UF membranes under low-pressure conditions; (ii) to assess the performance improvement with ferric ion and (iii) to examine flux behaviour, fouling development, and cleaning efficiency as key indicators of operational sustainability. By combining physical separation and chemical interaction mechanisms, this study aims to propose a practical and economically viable solution for V-contaminated waters.

Materials and methods

1Reagents, stock solutions and analysis

To create a synthetic solution, tap water and vanadium pentoxide (V_2O_5) were used. First, 0.0893 g of solid V_2O_5 was weighed and dissolved in a small amount of concentrated sulfuric acid (H_2SO_4) to create a V solution. Next, 50 mL of ultrapure water were added to the V solution to make a solution with a concentration of 1000 mg/L. This solution was then diluted with more water to make a final volume of 1 L, creating a stock solution with a concentration of 50 mg/L of V. From this stock solution, samples were taken and added to tap water to make synthetic solutions with different concentrations of V. The determination of V concentration was carried out with a Shimadzu 1800 UV–VIS spectrophotometer equipped with a 1.0 cm quartz cell. The analysis method used in the study (Heybeli et al. 2012) and the chemicals required for the analysis were carried out according to the method described here, but the measurement range was extended as a result of the method development. All the standard deviations reflect analytical repeatability based on measurement replicates rather than independent experimental repetitions. The water quality parameters of the tap water are given in Table 1.

$FeCl_3.6H_2O$ obtained from Merck was used for the preparation of ferrous coagulant. The prepared ferrous stock solution contained 2000 mg/L Fe concentration.

Membrane filtration system, membranes and operation

A laboratory-scale dead-end filtration setup with an effective membrane area of 14.6 cm^2 (Sterlitech) was used (Fig. 1). In the dead-end set up, pressure adjustments were made using inert nitrogen gas and the pressure was kept constant. The filtrate was measured with a computerized precision balance and the flux was calculated. The filtration cell consisted of an external 2.5 L reservoir and a dead-end filtration cell with a capacity of about 300 mL.

All experiments were performed at a constant temperature of 20 ± 1 °C. UP 150 (ultrafiltration) and MV020 (microfiltration) membranes from Microdyn-Nadir were used (Table 2). In

Table 1 Characteristics of tap water

Parameters	pH	Chloride mg/L	TOC mg/L	Sulfate mg/L	Conductivity µS/cm	Aluminum µg/L	Iron µg/L
Tap water	7.27	49.6	3.17	50.2	450	72.6	< 20

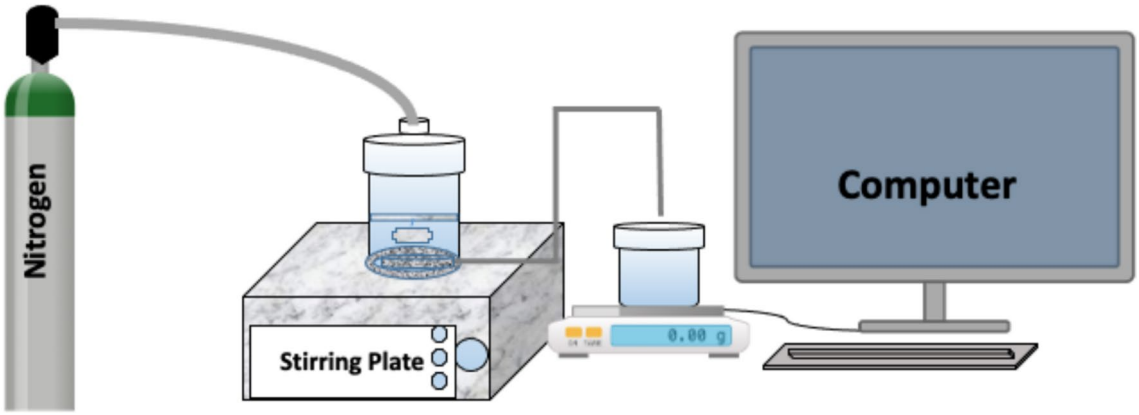


Fig. 1 Experimental set-up of the dead-end unit

the study with 1000 µg/L V-containing raw water, the experiments were also repeated by adding $FeCl_3$ to the 1000 µg/L V solution. The MV020 membrane was operated under 0.5, 1, 1.5 and 2 and the UP150 membrane was operated under 0.5, 1.5, 3 and 6 bar pressure. As a result of the processes, V removal and V concentrations in chemical cleaning water were analyzed.

Results and discussion

V removal studies

In the study, the initial concentration of V was 1 mg/L. $FeCl_3$ was added to the water to provide Fe/V ratios of 1 and 3. To clarify the role of $FeCl_3$ in enhancing V removal during membrane filtration, understanding the aqueous chemistry at neutral pH is crucial to elucidate $FeCl_3$'s enhancement mechanism. Under these conditions, V introduced as V_2O_5 predominantly dissolves to form monomeric vanadate species such as HVO_4^- and $H_2VO_4^-$, which are negatively charged and exhibit high aqueous solubility under neutral pH conditions. Simultaneously, $FeCl_3$ undergoes rapid hydrolysis, potentially generating amorphous $Fe(OH)_3$ flocs according to:

$$Fe^{3+} + 3\,H_2O \rightarrow Fe(OH)_3\,(s) + 3\,H^+$$

These $Fe(OH)_3$ particles may possess a net positive surface charge at neutral pH, thereby facilitating electrostatic adsorption of anionic vanadate ions:

$$Fe(OH)_3(s) + HVO_4^- \rightarrow Fe\text{-}V(s) + OH^-$$

Moreover, direct formation of sparingly soluble iron vanadate complexes such as FeVz(s) may occur:

$$Fe^{3+} + VO_4^{3-} \rightarrow FeVO_4(s)$$

These mechanisms convert dissolved V into particulate forms that are more effectively retained by membrane pores, particularly through size exclusion and physico-chemical entrapment. Thus, $FeCl_3$ enhancement not only improves V rejection in low-pressure membrane systems but also alters the dominant separation mechanism from molecular filtration to hybrid coagulation–filtration, with implications for both removal efficiency and fouling behavior. Experimental studies were carried out with synthetic solutions containing only V at different Fe/V ratios. The data for the optimization of the operating conditions for 1-h operation are given in Table 3.

As seen in Table 3, at different operating pressure values, V removal efficiencies in the range of 55.90–61.75% were obtained for UP150, while V removal efficiencies in the range of 18–24.50% were obtained for MV020. The V removal efficiency increased with the addition of $FeCl_3$ to the synthetic solution and the V removal efficiency for UP150 increased between 73.90% and 70.63% when the Fe/V ratio was 1, while the V removal efficiency for MV020 increased between 53.30% and 44.25% when the Fe/V ratio was 1. The results of the study show that increasing the

Table 2 Properties of the membranes used in the study

Membrane	Type	Materials	Pore size (µm)/Molecular Weight cut off (MWCO) (kDA)	pH range	Flux (LMH)	Contact angles (°)
UP150	Ultrafiltration (UF)	PES	150 kDA	1–14	≥ 285	64.95 ± 0.94
MV020	Microfiltration (MF)	PVDF	0.2 µm	2–11	≥ 700	64.86 ± 0.04

Table 3 V concentrations and removal efficiency in after membrane filtration

Membrane type	Fe/V ratio	Operating pressure	V removal, (init. conc. = 1 mg/L)	
		Bar	mg/L	%
MV020	–	0.5	0.755 ± 0.047	24.50 ± 6.23
		1	0.761 ± 0.031	23.90 ± 4.07
		1.5	0.768 ± 0.029	23.20 ± 3.78
		2	0.820 ± 0.045	18.00 ± 5.49
UP150	–	0.5	0.382 ± 0.024	61.75 ± 6.28
		1.5	0.394 ± 0.019	60.50 ± 4.82
		3	0.393 ± 0.031	60.60 ± 7.89
		6	0.440 ± 0.027	55.90 ± 6.14
MV020	1	0.5	0.467 ± 0.024	53.30 ± 5.14
		1	0.482 ± 0.023	51.70 ± 4.77
		1.5	0.518 ± 0.023	48.13 ± 4.44
		2	0.557 ± 0.036	44.25 ± 6.46
UP150	1	0.5	0.261 ± 0.013	73.90 ± 4.98
		1.5	0.263 ± 0.008	73.70 ± 3.04
		3	0.263 ± 0.012	73.65 ± 4.56
		6	0.293 ± 0.019	70.63 ± 6.48
MV020	3	0.5	0.398 ± 0.014	60.16 ± 3.52
		1	0.413 ± 0.015	58.70 ± 3.63
		1.5	0.435 ± 0.024	56.48 ± 5.52
		2	0.443 ± 0.024	55.62 ± 5.42
UP150	3	0.5	0.117 ± 0.008	88.28 ± 6.84
		1.5	0.119 ± 0.006	88.06 ± 5.04
		3	0.129 ± 0.006	87.05 ± 4.65
		6	0.140 ± 0.005	85.94 ± 3.57

Fe/V ratio has a positive effect on V uptake. When the Fe/V ratio was increased to 3, the V removal performance of UP150 increased between 88.28% and 85.94%, while the V removal performance of MV020 increased between 60.16% and 55.62% at the same Fe/V ratio. This positive effect was attributed to the assumption that Fe particles in the feed solution supplied a retention surface for V ions. The flux values of the optimization studies are given in Fig. 2.

As seen in Fig. 2, the flux values of UP150 membrane decreased from 627 to 496 LMH for the first 35 min at 6 bar pressure. After 35 min, the decrease in flux slowed. The flux values of MV020 membrane decreased from 1274 to 974 LMH in the first 30 min at 2 bar pressure. At the end of the next 30 min, it decreased to 899 LMH. At Fe/V:1 and Fe/V:3 ratios, the flux of UP150 membrane decreased rapidly in the first 40 min and the rate of decrease in flux slowed after the 40th min. Under 6 bar pressure, the flux value decreased from 598 to 402 LMH in the first 40 min when Fe/V ratio was 3. The flux value obtained at the end of the next 20 min of operation was 373 LMH. At Fe/V:1 and Fe/V:3 ratios, the flux of MV020 membrane decreased rapidly in the first 40 min and the rate of decrease in flux slowed after the 40th min. Under 2 bar pressure, the flux value decreased from 1055 to 730 LMH in the first 40 min when Fe/V ratio was 3. The flux value obtained at the end of the next 20 min of operation is 690 LMH. At other pressure values for all operating conditions and membranes, the flux values decreased rapidly at the beginning and the rate of decrease slowed after a certain period of time. Considering the flux and removal efficiencies, the UP150 membrane was operated for 6 h under 1.5 bar pressure at Fe/V:3 ratio and samples were taken at the end of each hour and V analyses were performed. The removal efficiencies and flux results of this study carried out under constant pressure are given in Table 4 and Fig. 3, respectively.

As seen in Table 4 V removal efficiency increased as the filtration time increased. The accumulation of iron particles on the membrane surface increased over time and this accumulation is presumed to enhance V removal efficiency due to increased interaction sites. At the end of 6-h of filtration, V concentration decreased from 1000 to 48 µg/L. As shown in Fig. 3, the flux value declined from 320 to 210 LMH during the initial 40 min of operation in the UP150 membrane throughout a 6-h period. Over a period of 240 min, the flux value declined to 177 LMH, and at 360 min, it reduced to 175 LMH.

Backwash of membranes

Subsequent to V treatment, the MV020 and UP150 membranes underwent chemical cleaning using acidic and basic solutions. Both membranes were subjected to a TMP of 1.5 bar and underwent three chemical cleaning cycles every 90 min. Following a 90-min period, the filtrate was collected and the concentration of V was measured. V removal and V concentrations in the backwash water were measured and are presented in Table 5.

Table 5 shows that there was no significant change in the V concentration in the filtrate after chemical cleaning in all experimental procedures. In addition V concentration the backwash water was quantified in every experiment. V concentration in the initial acidic backwash water without iron salt of the UP150 membrane was measured as 120 µg/L. The V concentration in the second backwash water was nearly equivalent to the values obtained in the first backwash. The concentration of V in the latest batch of acidic backwash water was measured as 145 µg/L. V concentration in the initial acidic backwash water without iron salt of the MV020 membrane was measured as 80 µg/L. The V concentration in the second backwash water yielded similar results to the first analysis, while the final analysis of the acidic backwash water showed a V concentration of 120 µg/L. For the UP150 membrane at an Fe/V ratio of 3, the V concentration of 186 µg/L in the initial acidic backwash water, 140 µg/L

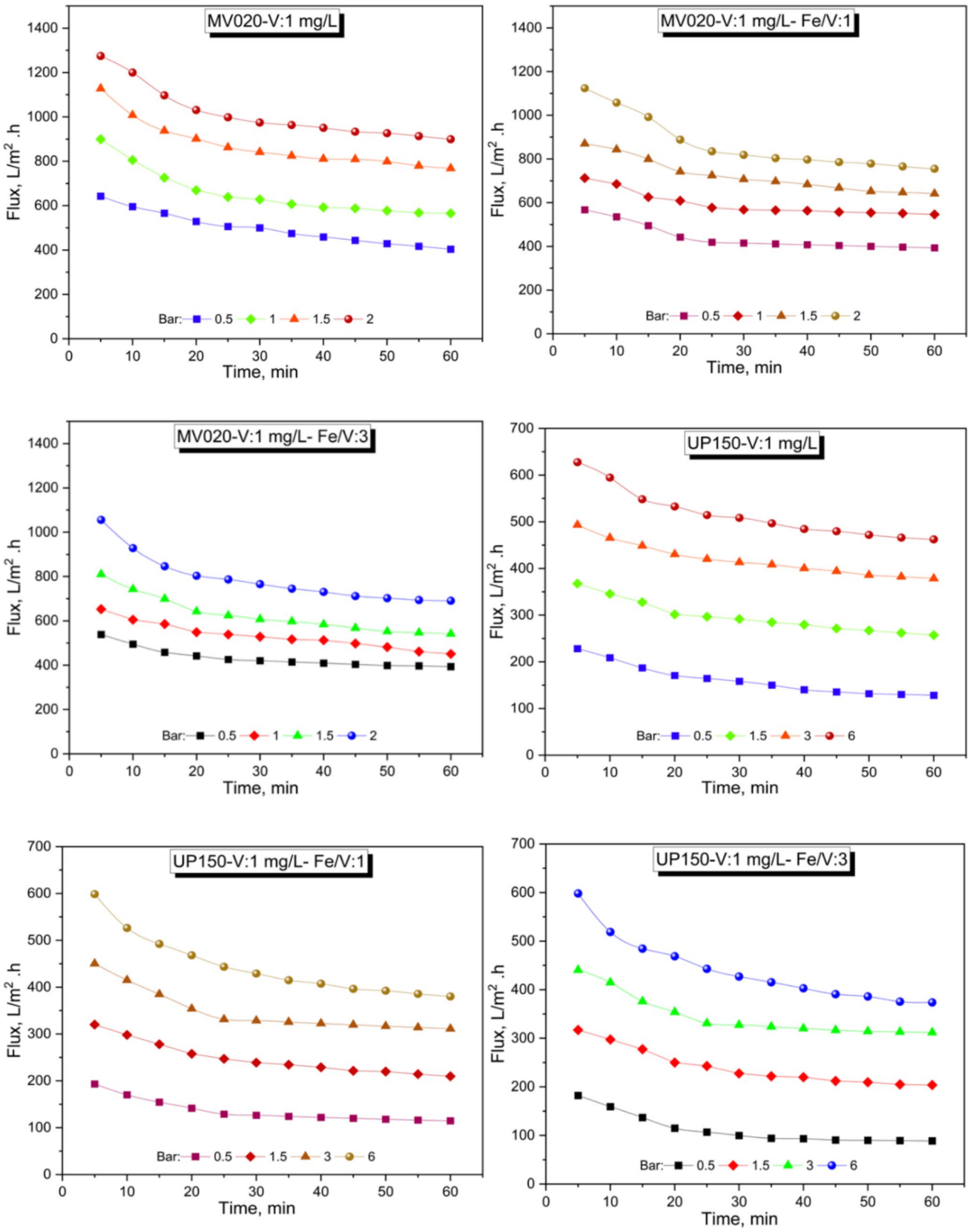


Fig. 2 Flux performance of MV020 and UP150 membranes at Fe/V ratios of 0, 1, and 3 over 60-min trials using 1 mg/L V-contaminated water. MV020 was tested at 0.5,1, 1.5 and 2 TMPs, and UP150 at 0.5, 1.5, 3 and 6 TMPs. The x-axis shows filtration time in minutes, and the left y-axis indicates flux (LMH)

Table 4 V removal with $FeCl_3$ at constant pressure

Membrane type	Fe/V ratio	Operating pressure	time	V removal, (init. conc. = 1 mg/L	
		Bar	hr	mg/L	%
UP150	3	1.5	1	0.116 ± 0.009	88,35 ± 7.76
		1.5	2	0.111 ± 0.009	88.89 ± 8.11
		1.5	3	0.107 ± 0.009	89.27 ± 8.41
		1.5	4	0.089 ± 0.006	91.05 ± 6.74
		1.5	5	0.069 ± 0.006	93.08 ± 8.70
		1.5	6	0.048 ± 0.005	95.14 ± 10.42

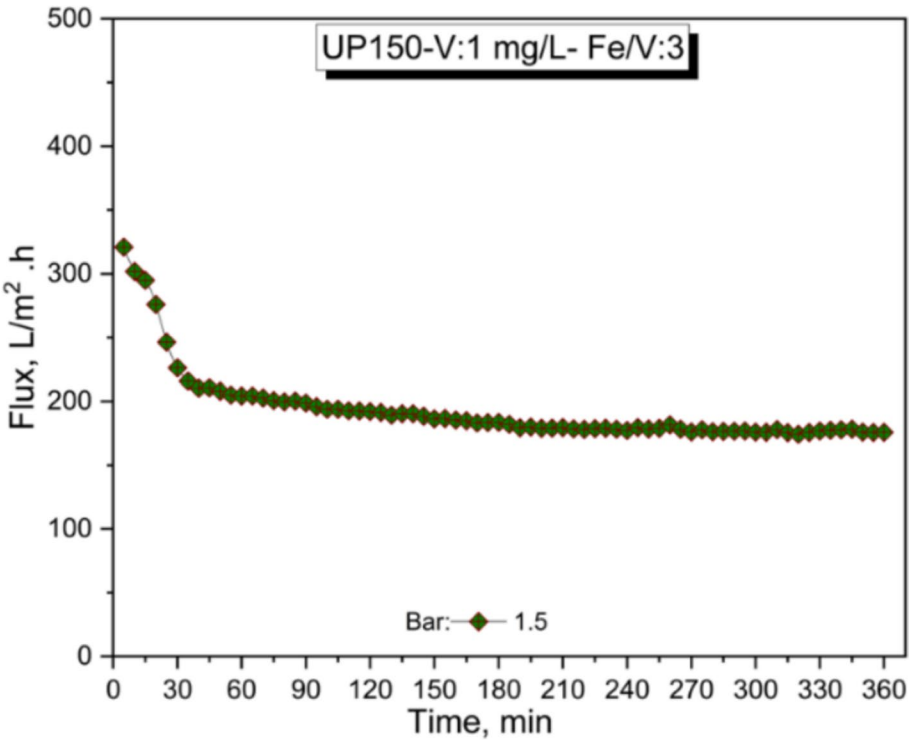


Fig. 3 Flux profile of the UP150 membrane over 6 h at 1.5 bar TMP in the presence of 1 mg/L V and Fe/V = 3. The x-axis shows filtration time in minutes, and the left y-axis indicates flux (LMH)

Table 5 V removal after chemical cleaning process

Membrane type	Fe/V ratio	Operating pressure	Time	V removal, (init. conc. = 1 mg/L)	
		Bar	min	mg/L	%
UP150	–	1.5	0–90	0.449 ± 0.015	55.08 ± 3.34
		1.5	90–180	0.414 ± 0.020	58.60 ± 4.83
		1.5	180–270	0.423 ± 0.020	57.71 ± 4.73
		1.5	270–360	0.440 ± 0.025	56.03 ± 5.68
MV020	–	1.5	0–90	0.778 ± 0.026	22,22 ± 3.34
		1.5	90–180	0.766 ± 0.033	23.39 ± 4.31
		1.5	180–270	0.771 ± 0.027	22.85 ± 3.50
		1.5	270–360	0.778 ± 0.034	22.22 ± 4.37
UP150	3	1.5	0–90	0.136 ± 0.009	86.31 ± 6.62
		1.5	90–180	0.137 ± 0.009	86.25 ± 6.57
		1.5	180–270	0.138 ± 0.010	86.13 ± 7.25
		1.5	270–360	0.139 ± 0.009	86,06 ± 6.47

in the subsequent acidic backwash water, and 123 µg/L in the final wash.

After each chemically backwash, flux was calculated and seen on Fig. 4.

Figure 4 and the accompanying data provide a comprehensive comparison of flux decline and cleaning recovery behaviour across three membrane configurations MV020 (Fe/V = 0), UP150 with ferric dosing (Fe/V = 3), and UP150 without coagulant (Fe/V = 0) operated under identical low-pressure conditions with 1 mg L^{-1} vanadium feed and periodic chemical back-washing every 90 min over a total of 6 h. This downward trajectory continued with each cycle, and by the end of the third cycle, the membrane recovered only 61% of its original flux, suggesting that the iron-based flocs induced more compact and strongly attached fouling layers that became increasingly resistant to chemical cleaning. In contrast, the same membrane operated without ferric enhancement displayed significantly better fouling resistance, with an initial flux of 390 LMH decreasing to 249 LMH in the first cycle, but recovering to 359 LMH after back-washing corresponding to a flux of 92%. This high recovery was maintained across subsequent cycles, with final recovery after six hours remaining at 85%, and the reversible fouling component consistently accounting for most of the total loss. This contrast indicates that while ferric addition improves V rejection (as discussed previously), it also contributes to irreversible pore blockage, especially in tight-pore membranes such as UP150, thereby shortening hydraulic service life unless more aggressive or frequent cleaning is employed. The MV020 membrane, with a larger nominal pore size and higher initial flux (1241 LMH), exhibited a relatively gentler but still substantial flux decline, recovering approximately 70% of its original flux after the third cleaning, suggesting that while its structure allows higher throughput, it is also more susceptible to deep-seated pore fouling in the absence of coagulation. Notably, the rate of flux recovery in MV020 also decreased across cycles, indicating increasing fouling compactness even without coagulant. The overall trends clearly show that the addition of Fe^{3+} leads to a greater irreversible fouling burden, especially in smaller-pore membranes, and that membrane morphology significantly influences both the severity and reversibility of fouling.

Membrane autopsy

The contact angle obtained after 6 h of operation of the membranes that were backwashed three times, FT-IR and SEM–EDS analyses were performed. Table 6 shows the contact angles of neat and used membranes operated with backwashing.

Analysis of the contact angles of the membranes presented in Table 6 reveals that accumulation occurs on the membrane, leading to an increase in the contact angles. This indicates that the hydrophobicity of the membranes increases, which indirectly indicates that the fluxes will also decrease. In addition, when a comparison was made between the MF and UF membranes the contact angle of membranes with smaller pore diameters increased more, possibly due to better V retention performance. The $FeCl_3$ added solution showed higher retention rate than the non-added solution, but a smaller increase in contact angle. SEM images are shown in Fig. 5, FTIR in Fig. 6 and EDS in Fig. 7.

Examination of the micrographs of neat membranes revealed that the MV020 membrane exhibited a more homogeneous and porous distribution than the UP150 membrane. In contrast deposits were more pronounced in the MV020 membrane than in the UP150 membrane. Furthermore, a comparison of the micrographs of the solution with $FeCl_3$ added to those without revealed a greater deposition in the former. The interpretation of these situation, in conjunction with the EDS and FTIR results, suggests that the deposition may account for the iron present on the surface.

Analysis of the spectra of the UP150 membrane revealed that the peaks ranged from 698 to 3400. The most significant peaks were recorded between 1000 and 1700. The peaks observed at 2926 and 3345 in this PES-based membrane may correspond to the stretching vibrations of the 2- and 3-bands of CH_3CH_2&CH. The peaks observed between 1485 and 1660 may result from C=C stretching vibrations (Coates 2004; Polat et al. 2020). Additionally, peaks at 1656 cm^{-1}, 1043 cm^{-1}, and 924 cm^{-1} signify the presence of sulfonic groups, associated with C=O bond stretching vibration. The reductions in these peaks suggest that the membrane structure is minimally impacted (Lu et al. 2017). The absence of the peak at 924 cm^{-1} in contaminated membranes may result from V-OH_2 stretching, suggesting the establishment of coordination bonds between vanadyl groups and V atoms (Abello et al. 1983; Petkov et al. 2002). Analysis of the MV020 membrane spectra revealed peaks ranging from 762 to 3371. The peak at 3371 cm^{-1} corresponds to the vibrations of the asymmetric and symmetric CH_2 group. The peak at 1403 cm^{-1} is associated with the fluctuation vibration of the CH_2 group, whereas the peak at 1180 cm^{-1} pertains to C–C bonds. The peaks identified at 975–762 cm^{-1} correspond to the α and β phases in PVDF membranes, while the peaks at 875–840 cm^{-1} are associated with asymmetric C–C–C and C–F stretching vibrations. The peak at 3371 cm^{-1} in the clean membrane likely indicates intermolecular O–H stretching associated with carboxyl, hydroxyl, and phenol groups. Additionally, the emergence of a new peak at 2931 cm^{-1} may be attributed to the stretching of the -CH_2 group influenced by the -OH (Coates 2004; Bai et al. 2012; Wang et al. 2014, 2015; Xue et al. 2015; Hu et al. 2016). The observed peak at 1648 cm^{-1} is likely attributable to C=C stretching vibration, as evidenced by the decrease

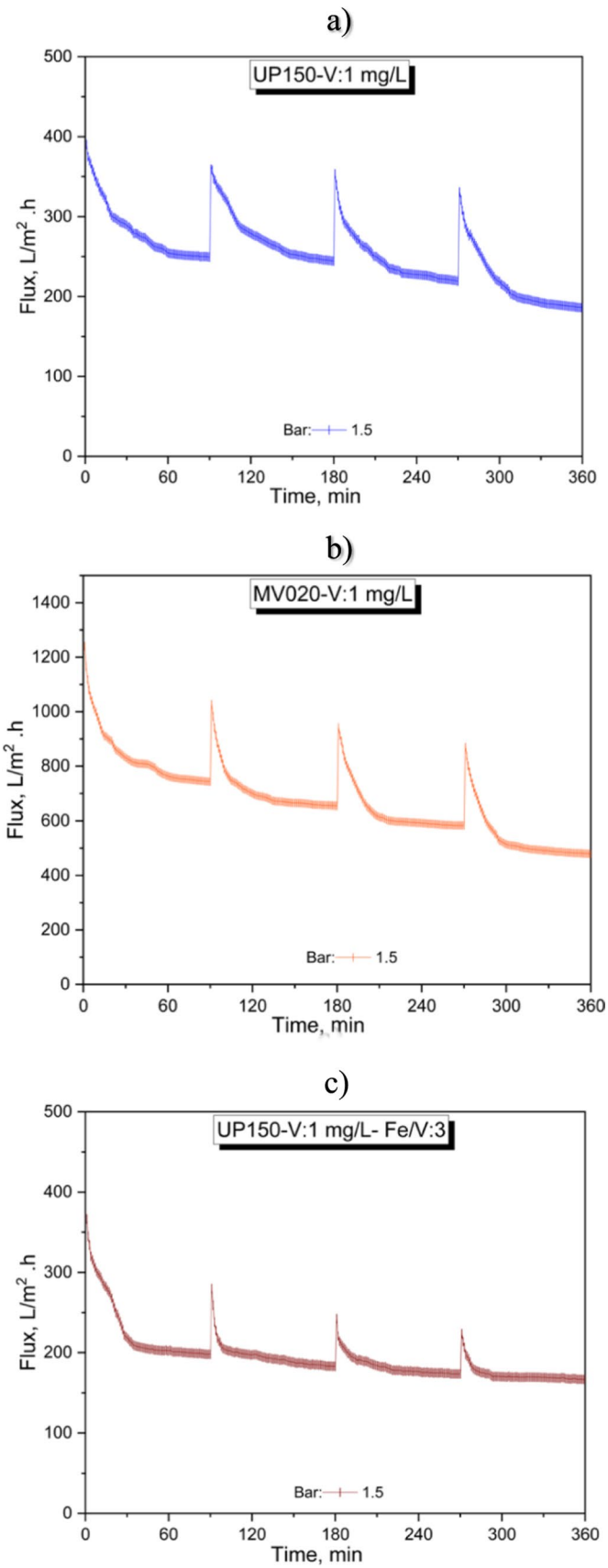


Fig. 4 Flux profiles of **a** MV020 and **b**, **c** UP150 membranes over 6-h filtration at 1.5 bar using 1 mg/L V solution. Backwashing was applied every 90 min. **a** and **b** were tested without $FeCl_3$ (Fe/V = 0), while **c** represents UP150 performance at Fe/V = 3. The x-axis shows time (min), and the y-axis indicates flux (LMH)

Table 6 Average contact angle value of membranes

Membrane	Average contact angle °
MV020 (Neat)	64.86 ± 0.04
MV020 (Used)	67.13 ± 1.84
UP150 (Neat)	64.95 ± 0.94
UP150 (Used)	87.36 ± 1.37
UP150—$FeCl_3$ (Used)	75.28 ± 2.33

in the EDS spectrum. The reduction in the stretching of the peak value at 975 cm^{-1} in the contaminated membrane may be associated with V–OH_2 stretching, indicating the formation of coordination bonds between vanadyl groups and V atoms (Abello et al. 1983; Petkov et al. 2002).

The examination of the EDS results indicates that the reduction in the F element ratio in the MV020 membrane may suggest a deterioration in the membrane's structural integrity. The observed increase in the distribution of certain elements across all membranes can be attributed to the characteristics of tap water. The characteristic Kα peak of V was detected at 4.96 keV, and a minor peak at this energy was observed when comparing fouled membranes with neat membranes. This phenomenon can be attributed to the relatively low initial concentration of V. Furthermore, reductions in the O element may be linked to oxidation processes.

Evaluation of operational sustainability and membrane longevity

Long-term performance assessments that couple extended-flux profiling with filtration characterisation reveal a clear trade-off between V rejection and membrane durability. SEM and EDS analyses revealed distinct morphological alterations and surface depositions, with more pronounced inorganic fouling observed on UP150 membranes enhanced with $FeCl_3$, supporting the notion of iron-induced compaction and accumulation. FTIR spectra further confirmed structural modifications via diminished sulfonic and fluorine-based functional group intensities, particularly in used membranes, indicating physicochemical interactions with V and iron species.

The contact angle measurements obtained for UP150 without $FeCl_3$ showed a notable increase from 64.95° to 87.36°, indicating a shift toward greater hydrophobicity over time. In contrast, the corresponding values for UP150 with $FeCl_3$ increased only to 75.28°. This difference may be attributed to the hydrophilic nature of $FeCl_3$, which likely contributed to the retention of more water-attracting surface characteristics by forming hydrated iron-vanadium complexes or residual salt layers that suppress the full hydrophobization of the membrane surface.

Flux recovery trends over repeated filtration and cleaning cycles corroborated these observations. UP150 with $FeCl_3$ showed a continuous decrease in flux recovery, retaining only 61% of its initial permeability after three chemical cleaning cycles, whereas UP150 without coagulant maintained 85% recovery, suggesting a predominance of reversible fouling. MV020, although initially exhibiting higher throughput, displayed decreasing recovery efficiency from 83 to 70% over time, reflecting a gradual increase in irreversible internal fouling.

From an environmental perspective, the backwashing streams generated during membrane operation contain V and iron species released from the membrane surface. While these streams represent secondary waste flows that may require appropriate management. If necessary, backwashing streams could be further concentrated using additional separation processes, enabling subsequent recovery or targeted treatment of accumulated metals. Consequently, incorporation of backwash stream management into overall process design is an important aspect of sustainable membrane operation.

Collectively, these findings confirm that $FeCl_3$-assisted filtration can more than double V rejection yet accelerates irreversible fouling and surface ageing, shortening hydraulic service life unless cleaning chemistry, frequency, or membrane surface properties are further optimised. Therefore, future designs should balance ferric dose with targeted cleaning protocols or adopt fouling-resistant coatings to sustain operational sustainability and membrane longevity under real-world, low-pressure conditions.

Energy consumption

Operational sustainability in low-pressure membrane systems is governed not only by contaminant removal efficiency but also by energy demand, chemical consumption, and long-term hydraulic performance under continuous operation. In this context, the UP150 UF membrane operated at 1.5 bar with ferric enhancement was selected as the representative condition for evaluating process sustainability. To evaluate the economic and operational feasibility of the process, the Specific Energy Consumption (SEC) was estimated for the UP150 membrane during the 6-h filtration period at a Fe/V ratio of 3 and a constant TMP of 1.5 bar. Following the methodology for dead-end filtration systems, the energy consumption (E) was calculated based on the hydraulic work performed over the total permeate volume (Vtotal), assuming a standard pump efficiency (η_P) of 0.7. The SEC, representing the energy required to produce a unit volume of treated water (kWh/m^3), was determined using the following expression (Blankert et al. 2007):

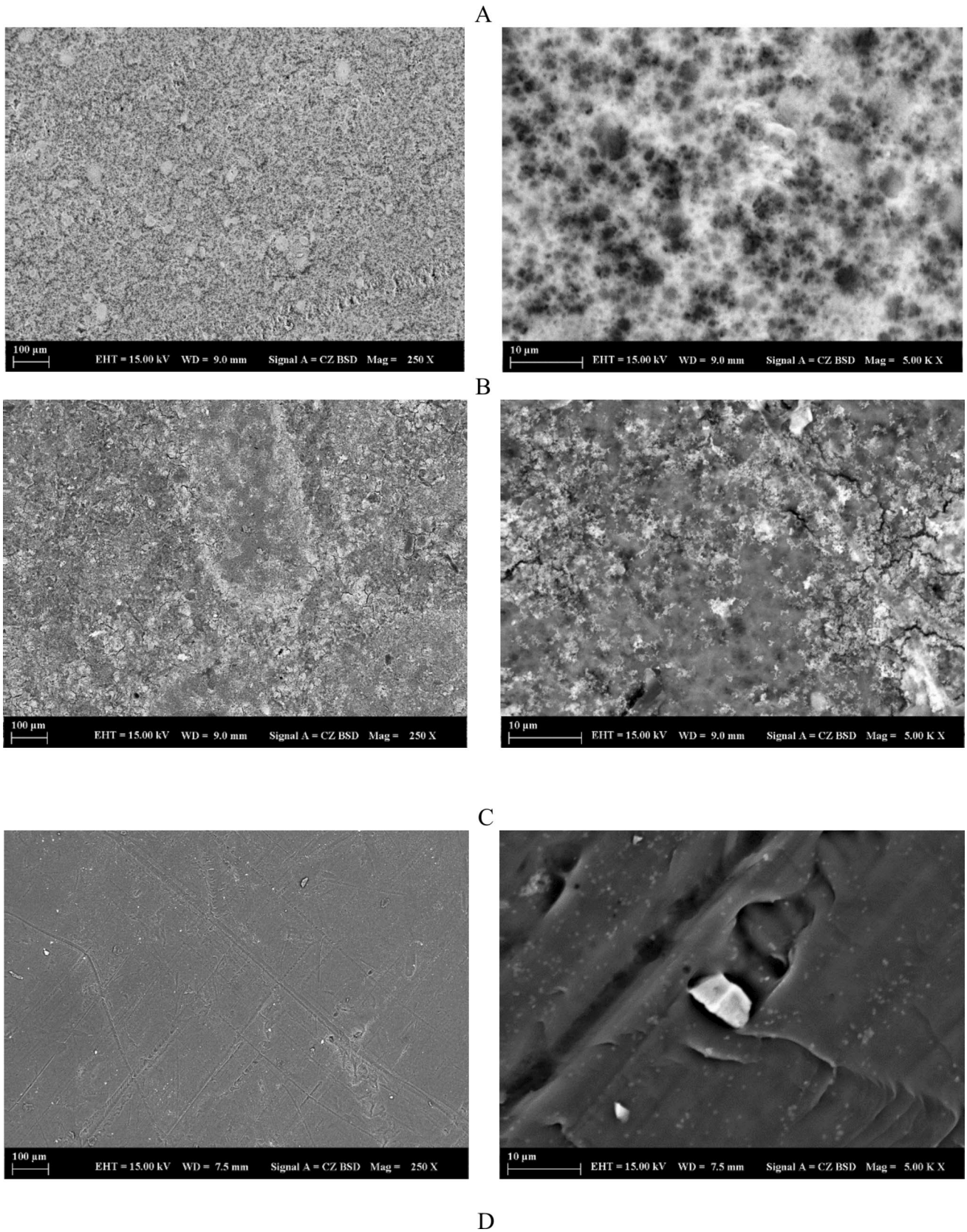


Fig. 5 SEM: **A** Neat MV020 membrane 5000(right) and 250(left) magnification, **B** Used MV020 membrane 5000(right) and 250(left) magnification, **C** Neat UP150 membrane 5000(right) and 250(left magnification, **D** Used UP150 membrane 5000(right) and 250(left) magnification, **E** Used UP150 membrane assisted FeCl3 5000(right) and 250(left) magnification,

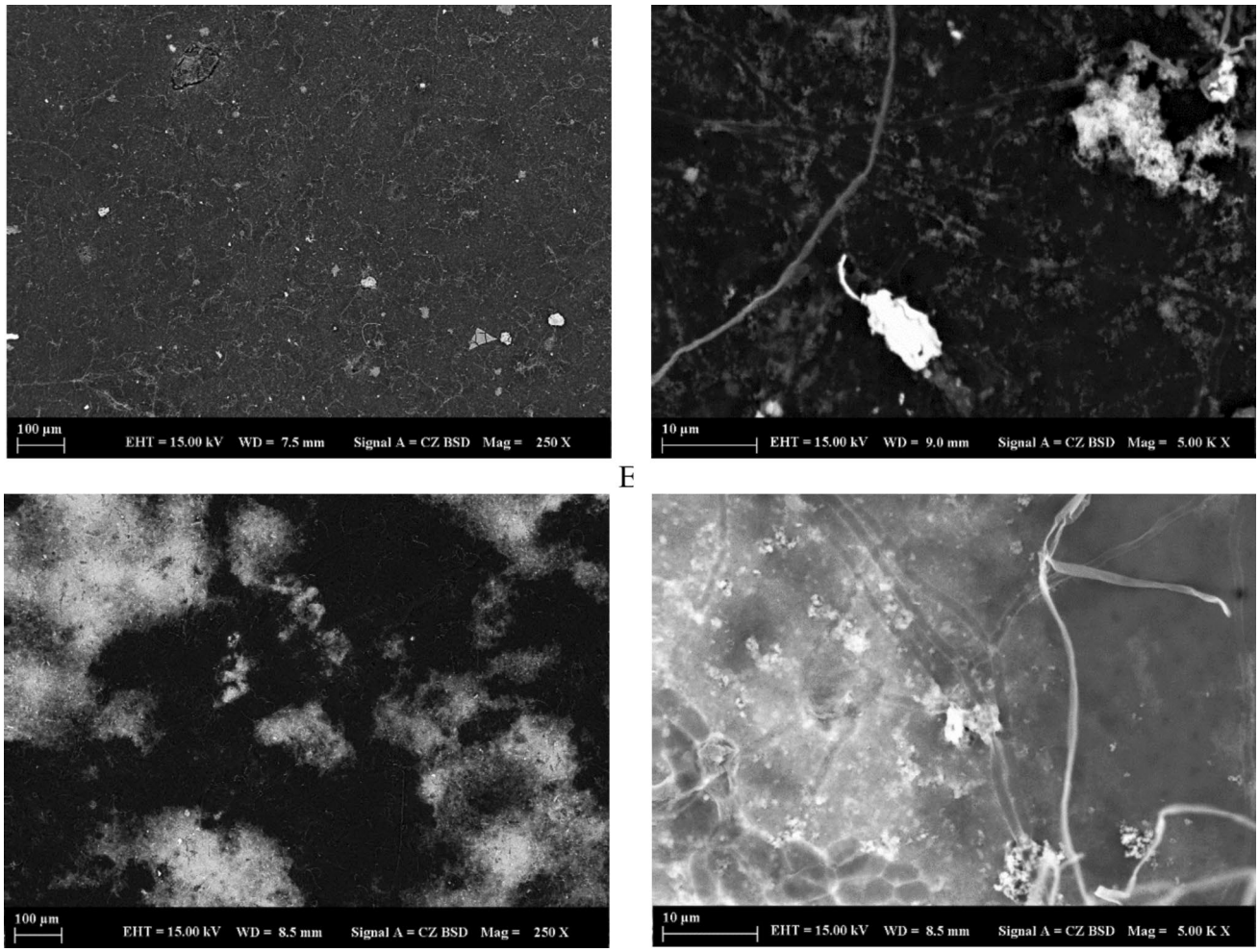


Fig. 5 (continued)

$$SEC(\mathrm{kWh.m^{-3}}) = \frac{\Delta P}{\eta_P(3.6x10^6)}$$

Under the operating conditions of 1.5 bar, the SEC was calculated to be approximately 0.0595 kWh/m^3. Throughout the 6-h operation, the flux value declined significantly from an initial 320 LMH to 175 LMH due to the progressive accumulation of Fe–V complexes on the membrane surface. Despite this flux decline, the total permeate volume collected during the cycle was approximately 1.713 L. Consequently, the total energy consumption (Etotal) for the duration of the 6-h cycle was determined by multiplying the SEC by the total permeate volume (Vtotal) obtained through the integration of the flux-time profile. Which resulted in a total energy expenditure of 0.102 Wh for the laboratory scale unit. Overall, the calculated SEC value confirms the low hydraulic energy demand characteristic of low-pressure membrane operation. In addition to electrical energy consumption, the applied ferric dose contributes to the overall operating cost. However, the level of chemical consumption remains relatively modest when compared to the substantial enhancement achieved in V rejection, indicating a favorable trade-off between operational input and treatment performance. A wide range of physicochemical and biological techniques has been investigated for V removal from aqueous systems, including adsorption, chemical precipitation, biological processes, solvent extraction, photocatalytic reduction, electrokinetic approaches, and coagulation-based treatments. Among these alternatives, adsorption and biologically driven processes stand out due to their relatively low energy requirements coupled with satisfactory V removal efficiencies, making them particularly attractive for sustainable water treatment applications (Peng et al. 2022). By contrast, pressure-driven membrane processes generally require higher hydraulic energy input, especially under the elevated operating pressures typical of RO/NF. For example, Hafiz et al. reported that, depending on the applied pressure and recovery, the SEC ranged from 0.46 to 0.73 kWh m^{-3} for RO and from 0.68 to 2.35 kWh m^{-3}

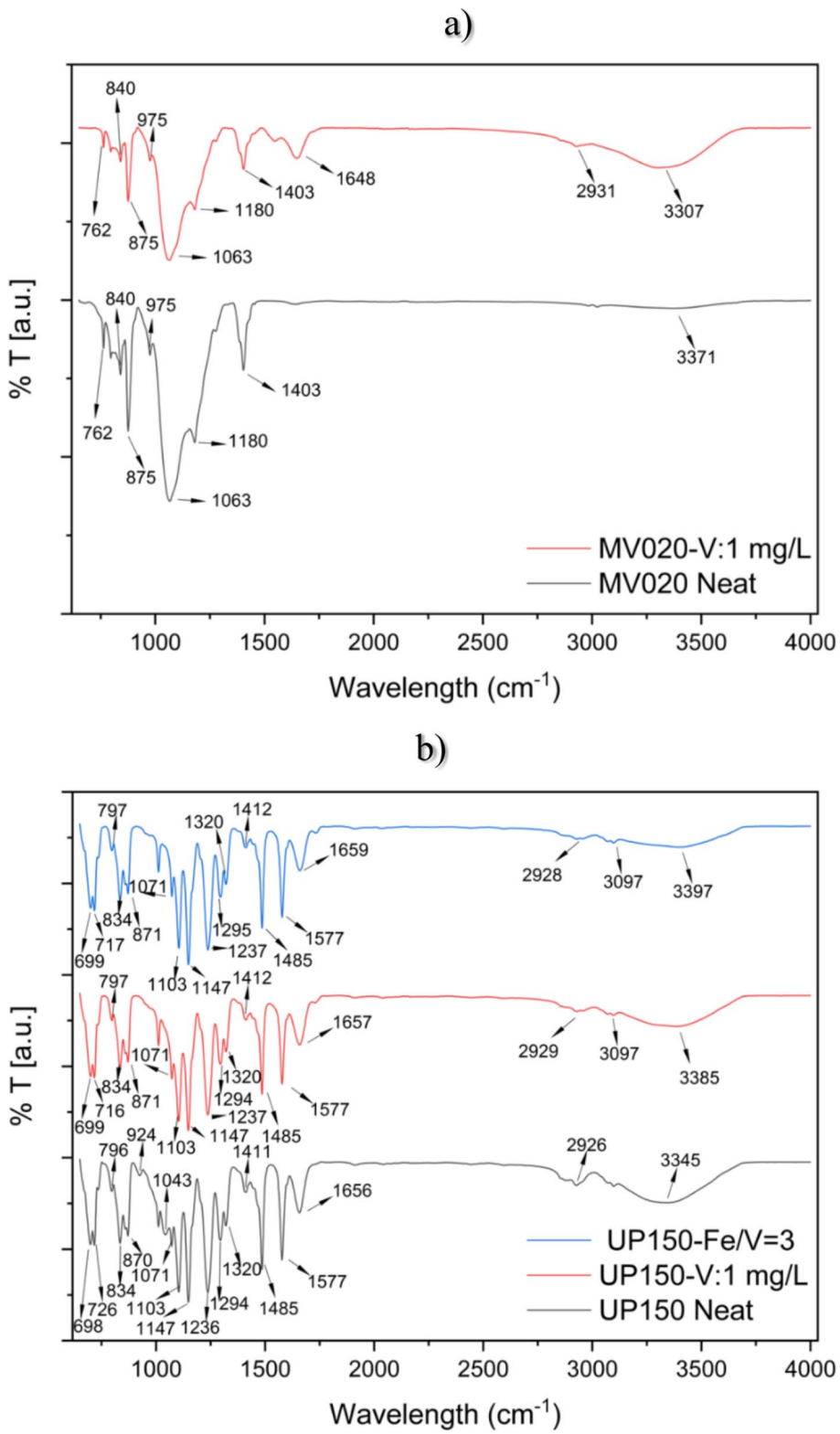


Fig. 6 FTIR spectra of neat and dirty a) MV020 and b) UP150 membranes

for NF (Hafiz et al. 2021). In the present study, the SEC obtained at an applied pressure of 1.5 bar was considerably lower, underscoring the favorable energy profile of the proposed low-pressure membrane operation. This reduced hydraulic energy requirement suggests a promising operational cost advantage, particularly when combined with ferric-assisted vanadium removal.

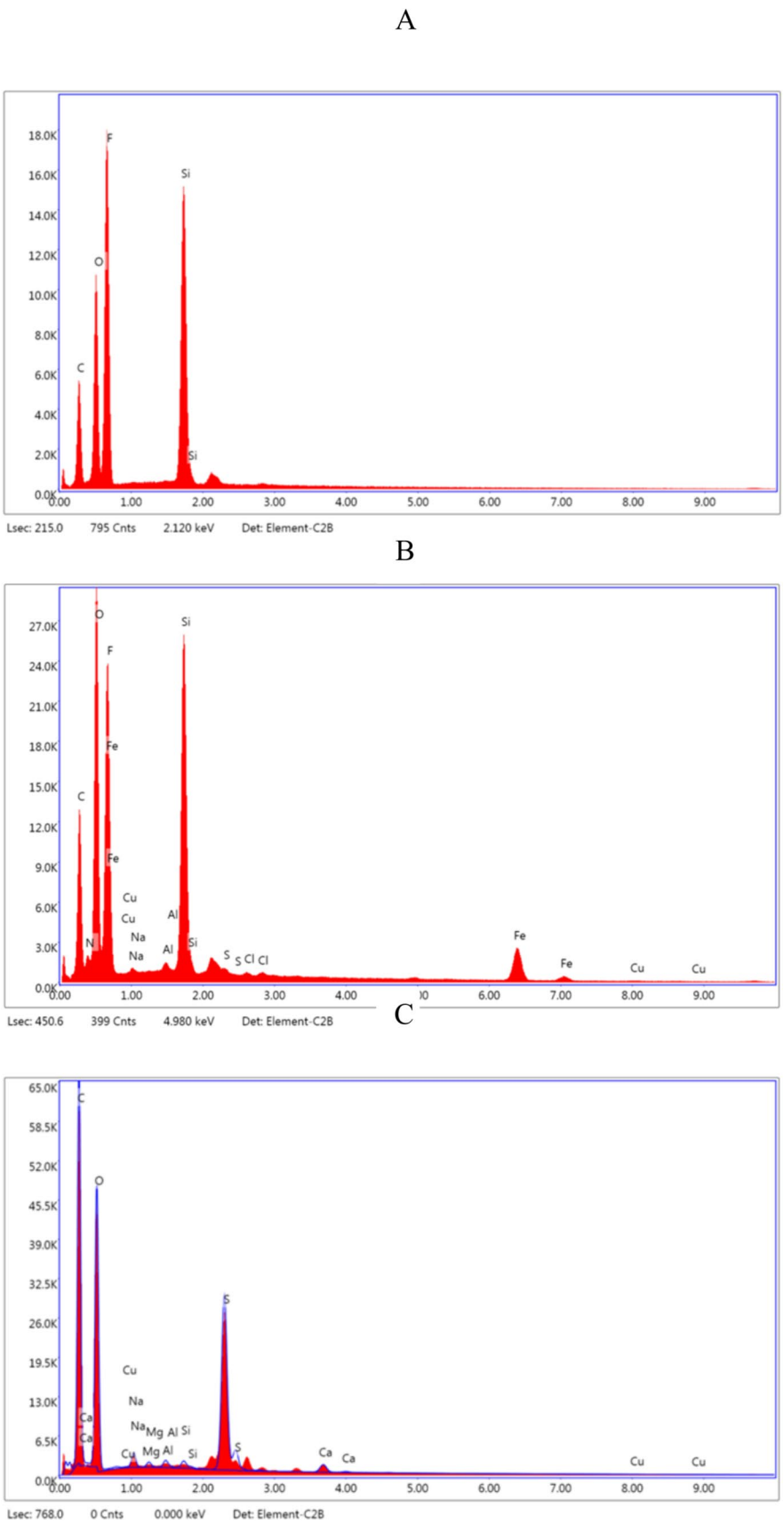
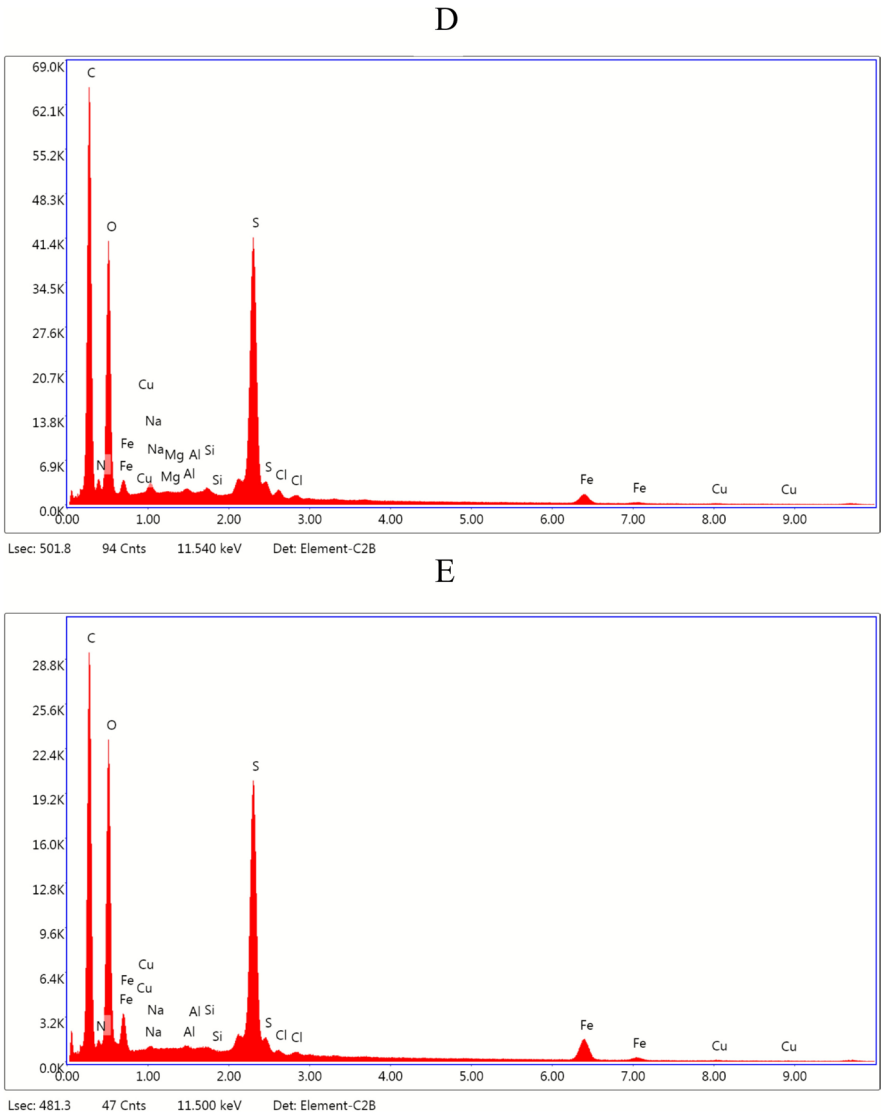


Fig. 7 EDS: **A** Neat MV020 membrane, **B** Used MV020 membrane, **C** Neat UP150 membrane, **D** Used UP150 membrane, **E** Used UP150 membrane assisted $FeCl_3$

Fig. 7 (continued)



Conclusion

This study demonstrated that low-pressure membrane filtration can be an effective approach for V removal from water, particularly when enhanced with $FeCl_3$. While unassisted MF and UF membranes exhibited limited intrinsic V rejection, ferric addition substantially improved removal performance, with the UP150 membrane achieving removal efficiencies exceeding 90% under optimized conditions (Fe/V = 3, 1.5 bar). These results indicate that coagulant assisted low-pressure UF has the potential to meet emerging drinking water targets for V while operating under moderate hydraulic conditions. However, enhanced removal efficiency was accompanied by increased fouling severity and reduced flux recovery, especially for tight-pore UF membranes. Repeated chemical cleaning cycles revealed a progressive increase in irreversible fouling when ferric dosing was applied, indicating that long-term membrane performance is sensitive to coagulant induced deposition. In contrast, membranes operated without ferric addition exhibited more stable hydraulic behaviour but lower removal efficiency. These findings highlight the importance of balancing ferric dosage with membrane selection and cleaning frequency to maintain an acceptable membrane lifespan.

The SEC calculated for the optimal membrane and operating condition (UP150 at 1.5 bar, approximately 0.06 kWh m^{-3}) confirms the low hydraulic energy requirement of the process. Nevertheless, the associated flux decline and increased fouling demonstrate that energy efficiency alone is insufficient to ensure overall operational sustainability.

The use of tap water as the feed matrix in the experimental studies, while not fully representative of raw surface or groundwater, demonstrates that V removal remains effective in the presence of background ions and organic matter. However, increasing concentrations of coexisting ions commonly present in natural waters may significantly influence

Fe^{3+} hydrolysis, floc formation, V speciation, and fouling behaviour, and thus should be carefully considered when extending the process to more complex water matrices.

Overall, the results indicate that ferric-assisted low-pressure UF can achieve high V removal at low hydraulic energy demand. However, flux decline and membrane fouling limit its suitability as a standalone long-term solution. Nevertheless, the findings provide valuable insight into ferric assisted removal mechanisms and suggest that alternative or hybrid treatment strategies that decouple high removal efficiency from severe membrane fouling may offer more practical pathways for future process development.

Acknowledgements We acknowledge the efforts of our research team members from Yildiz Technical University for their valuable input and cooperation throughout this article.

Funding Open access funding provided by the Scientific and Technological Research Council of Türkiye (TÜBİTAK).

Declarations

Conflict of interest The authors declare that they have no known competing financial interests or personal relationships that could have appeared to influence the work reported in this paper.

Open Access This article is licensed under a Creative Commons Attribution 4.0 International License, which permits use, sharing, adaptation, distribution and reproduction in any medium or format, as long as you give appropriate credit to the original author(s) and the source, provide a link to the Creative Commons licence, and indicate if changes were made. The images or other third party material in this article are included in the article's Creative Commons licence, unless indicated otherwise in a credit line to the material. If material is not included in the article's Creative Commons licence and your intended use is not permitted by statutory regulation or exceeds the permitted use, you will need to obtain permission directly from the copyright holder. To view a copy of this licence, visit http://creativecommons.org/licenses/by/4.0/.

References

Abello L, Husson E, Repelin Y, Lucazeau G (1983) Vibrational spectra and valence force field of crystalline V2O5. Spectrochim Acta A Mol Biomol Spectrosc 39:641–651. https://doi.org/10.1016/0584-8539(83)80040-3

Al-Jaser ZA, Hamoda MF (2019) Removal of nickel and vanadium from desalination brines by ion-exchange resins. Desalin Water Treat 157:148–156. https://doi.org/10.5004/dwt.2019.24127

ATSDR (2012) U.S. Department of health and human services public health service. agency for toxic substances and disease registry. Toxicological Profile for Vanadium

Bahr C, Jekel M, Amy G (2022) Vanadium removal from drinking water by FIXED-BED adsorption on granular ferric hydroxide. AWWA Water Sci 4:e127z1. https://doi.org/10.1002/aws2.1271

Bai H, Wang X, Zhou Y, Zhang L (2012) Preparation and characterization of poly(vinylidene fluoride) composite membranes blended with nano-crystalline cellulose. Progress Nat Sci: Mater Int 22:250–257. https://doi.org/10.1016/j.pnsc.2012.04.011

Barceloux DG, Barceloux D (1999) Vanadium. J Toxicol Clin Toxicol 37:265–278. https://doi.org/10.1081/CLT-100102425

Bera SP, Godhaniya M, Kothari C (2022) Emerging and advanced membrane technology for wastewater treatment: a review. J Basic Microbiol 62:245–259. https://doi.org/10.1002/jobm.202100259

Blankert B, Kattenbelt C, Betlem BHL, Roffel B (2007) Dynamic optimization of a dead-end filtration trajectory: non-ideal cake filtration. J Membr Sci 290:114–124. https://doi.org/10.1016/j.memsci.2006.12.024

Chen L, Liu F, Li D (2011) Precipitation of crystallized hydrated iron(III) vanadate from industrial vanadium leaching solution. Hydrometallurgy 105:229–233. https://doi.org/10.1016/j.hydromet.2010.10.002

Cintas P (2004) The road to chemical names and eponyms: discovery, priority, and credit. Angew Chem Int Ed Engl 43:5888–5894. https://doi.org/10.1002/anie.200330074

Coates J (2004) Encyclopedia of Analytical Chemistry -IInterpretation of Infrared Spectra, A Practical Approach. 1–23

Dong Y, Qiao Y, Zhang P et al (2024) Insights into vanadium removal performance and mechanism in aqueous solution by one-step pyrolysis prepared Phytolacca acinosa biochar composite. J Mol Liq 411:125752. https://doi.org/10.1016/j.molliq.2024.125752

Gao Y, Jiang J, Tian S et al (2017) BOF steel slag as a low-cost sorbent for vanadium (V) removal from soil washing effluent. Sci Rep 7:11177. https://doi.org/10.1038/s41598-017-11682-3

Gillio Meina E (2020) The Influence Of Water Qualıty Characterıstıcs On Vanadıum Toxıcıty To Model Aquatıc Organısms. University of Saskatchewan

Gillio Meina E, Raes K, Liber K (2019) Models for the acute and chronic aqueous toxicity of vanadium to *Daphnia pulex* under a range of surface water chemistry conditions. Ecotoxicol Environ Saf 179:301–309. https://doi.org/10.1016/j.ecoenv.2019.04.052

Gurjar VR, Koujalagi PS, Revankar HN, Kulkarni RM (2022) Adsorptive removal of vanadium from aqueous media by ion exchange resin. Emergent Mater 5:1543–1551. https://doi.org/10.1007/s42247-021-00251-0

Hafiz M, Hawari AH, Alfahel R et al (2021) Comparison of nanofiltration with reverse osmosis in reclaiming tertiary treated municipal wastewater for irrigation purposes. Membranes 11:32. https://doi.org/10.3390/membranes11010032

Hao L, Liu Y, Chen N et al (2021) Microbial removal of vanadium (V) from groundwater by sawdust used as a sole carbon source. Sci Total Environ 751:142161. https://doi.org/10.1016/j.scitotenv.2020.142161

Heybeli G, Basaran A, Elçi L (2012) Spectrophotometric method for determination and speciation of vanadium in various samples. Anal Chem Lett 2:63–71. https://doi.org/10.1080/22297928.2012.10648253

Hu L, Zeng G, Chen G et al (2016) Treatment of landfill leachate using immobilized *Phanerochaete chrysosporium* loaded with nitrogen-doped TiO 2 nanoparticles. J Hazard Mater 301:106–118. https://doi.org/10.1016/j.jhazmat.2015.08.060

Judd SJ (2017) Membrane technology costs and me. Water Res 122:1–9. https://doi.org/10.1016/j.watres.2017.05.027

Lin J-Y, Mahasti NNN, Huang Y-H (2021) Recent advances in adsorption and coagulation for boron removal from wastewater: a comprehensive review. J Hazard Mater 407:124401. https://doi.org/10.1016/j.jhazmat.2020.124401

Liu H, Zhang B, Yuan H et al (2017) Microbial reduction of vanadium (V) in groundwater: interactions with coexisting common electron acceptors and analysis of microbial community. Environ Pollut 231:1362–1369. https://doi.org/10.1016/j.envpol.2017.08.111

Liu J, Huang Y, Li H, Duan H (2022) Recent advances in removal techniques of vanadium from water: a comprehensive review. Chemosphere 287:132021. https://doi.org/10.1016/j.chemosphere.2021.132021

Lu R, Zhang C, Piatkovsky M et al (2017) Improvement of virus removal using ultrafiltration membranes modified with grafted zwitterionic polymer hydrogels. Water Res 116:86–94. https://doi.org/10.1016/j.watres.2017.03.023

Ma J, Li Y, Wang C-C, Wang P (2023) Superior removal of Vanadium(V) from simulated groundwater with a Fe-based metal-organic framework immobilized on cotton fibers. Langmuir 39:16863–16872. https://doi.org/10.1021/acs.langmuir.3c02411

Mahdavi M, Amin MM, Mahvi AH et al (2018) Metals, heavy metals and microorganism removal from spent filter backwash water by hybrid coagulation-UF processes. J Water Reuse Desalin 8:225–233. https://doi.org/10.2166/wrd.2017.148

Mamane Y, Pirrone N, Nriagu J (1998) Vanadium in the environment. John Wiley, New York, pp 37–71

Meng R, Chen T, Zhang Y et al (2018) Development, modification, and application of low-cost and available biochar derived from corn straw for the removal of vanadium(v) from aqueous solution and real contaminated groundwater. RSC Adv 8:21480–21494. https://doi.org/10.1039/C8RA02172D

Moreira VR, Costa FCR, Moser PB et al (2023) Ultrafiltration with in-line coagulation (FeCl3) to enhance arsenic removal and improve drinking water quality: from bench to pilot-scale. Chem Eng J 472:145063. https://doi.org/10.1016/j.cej.2023.145063

Obotey Ezugbe E, Rathilal S (2020) Membrane technologies in wastewater treatment: a review. Membranes 10:89. https://doi.org/10.3390/membranes10050089

Ohwobete JE, Latta DE, Hoffman AR et al (2025) Well exposed: exploring the chemical and microbial composition in well and municipal drinking waters in Iowa. Environ Sci Water Res Technol 11:2017–2034. https://doi.org/10.1039/D5EW00216H

Peng H, Guo J, Li B et al (2022) Removal and recovery of vanadium from waste by chemical precipitation, adsorption, solvent extraction, remediation, photo-catalyst reduction and membrane filtration. A review. Environ Chem Lett 20:1763–1776. https://doi.org/10.1007/s10311-022-01395-z

Petkov V, Trikalitis PN, Bozin ES et al (2002) Structure of $V_2 O_5 \cdot n H_2 O$ xerogel solved by the atomic pair distribution function technique. J Am Chem Soc 124:10157–10162. https://doi.org/10.1021/ja026143y

Polat B, Ozay Y, Bilici Z et al (2020) Membrane modification with semiconductor diode laser to reduce membrane biofouling for external MBR system and modelling study. Sep Purif Technol 241:116747. https://doi.org/10.1016/j.seppur.2020.116747

Rehder D (2015) The role of vanadium in biology. Metallomics 7:730–742. https://doi.org/10.1039/C4MT00304G

Richardson SD, Manasfi T (2024) Water analysis: emerging contaminants and current issues. Anal Chem 96:8184–8219. https://doi.org/10.1021/acs.analchem.4c01423

Roccaro P, Vagliasindi FGA (2015) Coprecipitation of vanadium with iron(III) in drinking water: a pilot-scale study. Desalin Water Treat 55:799–809. https://doi.org/10.1080/19443994.2014.942381

Rout PC, Sarangi K (2014) Separation of vanadium using both hollow fiber membrane and solvent extraction technique—a comparative study. Sep Purif Technol 122:270–277. https://doi.org/10.1016/j.seppur.2013.11.010

Rudin NA, Achimugu S, Saha AK (2021) Application of cell membrane principles in molecular separation process with membrane technology on food science. ICSE 4:306–310

Salehi S, Alijani S, Anbia M (2020) Enhanced adsorption properties of zirconium modified chitosan-zeolite nanocomposites for vanadium ion removal. Int J Biol Macromol 164:105–120. https://doi.org/10.1016/j.ijbiomac.2020.07.055

Sefström NG (1831) Ueber das Vanadin, ein neues Metall, gefunden im Stangeneisen von Eckersholm, einer Eisenhütte, die ihr Erz von Taberg in Småland bezieht. Ann Phys (Berl) 97:43–49. https://doi.org/10.1002/andp.18310970103

Shang G, Zhang G, Gao C et al (2014) A novel nanofiltration process for the recovery of vanadium from acid leach solution. Hydrometallurgy 142:94–97. https://doi.org/10.1016/j.hydromet.2013.11.007

Shon HK, Vigneswaran S, Ngo HH, Ben Aim R (2005) Is semi-flocculation effective as pretreatment to ultrafiltration in wastewater treatment? Water Res 39:147–153. https://doi.org/10.1016/j.watres.2004.09.003

Simandl GJ, Paradis S (2022) Vanadium as a critical material: economic geology with emphasis on market and the main deposit types. Appl Earth Sci 131:218–236. https://doi.org/10.1080/25726838.2022.2102883

Tan L, Liu T, Zhang Y et al (2023) Enhance selective separation of vanadium and iron from acid-leaching solution with sulfamic acid modified resin. Chem Eng J 457:141286. https://doi.org/10.1016/j.cej.2023.141286

Vasseghian Y, Sadeghi Rad S, Vilas-Boas JA, Khataee A (2021) A global systematic review, meta-analysis, and risk assessment of the concentration of vanadium in drinking water resources. Chemosphere 267:128904. https://doi.org/10.1016/j.chemosphere.2020.128904

Wang B-Y, Tseng CK, Shih C-M et al (2014) Polytetrafluoroethylene (PTFE)/silane cross-linked sulfonated poly(styrene–ethylene/butylene–styrene) (sSEBS) composite membrane for direct alcohol and formic acid fuel cells. J Membr Sci 464:43–54. https://doi.org/10.1016/j.memsci.2014.03.076

Wang F, Zhu H, Zhang H et al (2015) Effect of surface hydrophilic modification on the wettability, surface charge property and separation performance of PTFE membrane. J Water Process Eng 8:11–18. https://doi.org/10.1016/j.jwpe.2015.08.004

Xue Y, Zhao H, Ge L et al (2015) Comparison of the performance of waste leachate treatment in submerged and recirculated membrane bioreactors. Int Biodeterior Biodegrad 102:73–80. https://doi.org/10.1016/j.ibiod.2015.01.005

Zhu H, Xiao X, Guo Z et al (2018) Adsorption of vanadium (V) on natural kaolinite and montmorillonite: characteristics and mechanism. Appl Clay Sci 161:310–316. https://doi.org/10.1016/j.clay.2018.04.035

Zulu B, Oyewo OA, Sithole B et al (2020) Functionalized sawdust-derived cellulose nanocrystalline adsorbent for efficient removal of vanadium from aqueous solution. Front Environ Sci 8:56. https://doi.org/10.3389/fenvs.2020.00056

Publisher's Note Springer Nature remains neutral with regard to jurisdictional claims in published maps and institutional affiliations.